

# The relation between extended radio and line emission for radio-loud quasars

Xinwu Cao<sup>1,2</sup> and D. R. Jiang<sup>1</sup>

1. *Shanghai Astronomical Observatory, Chinese Academy of Sciences, Shanghai, 200030, China*

and *National Astronomical Observatories, Chinese Academy of Sciences, China, cxw@center.shao.ac.cn*

2. *Beijing Astrophysical Center(BAC), Beijing, China*

Accepted . Received ; in original form

## ABSTRACT

We explore the relationship between the extended radio and line emission for a radio-loud quasar sample including both core-dominated and lobe-dominated quasars. A strong correlation is present between the extended radio and broad-line emission. The core emission is also correlated with the broad-line emission for core-dominated quasars in the sample. The statistic behaviour on the core emission of lobe-dominated quasars is rather different from that of core-dominated quasars. The extended radio luminosity is a good tracer for jet power, while the core luminosity can only be a jet power tracer for core-dominated quasars.

**Key words:** galaxies:active– galaxies:jets–quasars:emission lines

## 1 INTRODUCTION

The current most favoured models of powering active galactic nuclei (AGNs) involve gas accretion onto a massive black hole, though the details are still unclear. Relativistic jets have been observed in many radio-loud AGNs and are believed to be formed very close to the black holes. In some theoretical models of the formation of the jet, the power is generated through accretion and then extracted from the disc/black hole rotational energy and converted into the kinetic power of the jet (Blandford & Znajek; Blandford & Payne 1982). Recently, numerical simulations show that the jet can be accelerated from the disk region very close to the black hole (Koide et al. 1999). The jet-disc connection has been investigated by many workers (Rawlings & Saunders 1991; Falcke & Biermann 1995; Xu & Livio 1999). An effective approach to study the link between these two phenomena is to explore the relationship between the corresponding emission. A strong correlation is found between the low-frequency radio and narrow line luminosities of 3C radio sources (Baum & Heckman 1989; Rawlings et al. 1989; McCarthy 1993; Tadhunter et al. 1998). The bulk kinetic power in the jet  $Q_{\text{jet}}$  can be inferred from its low-frequency radio luminosity. Rawlings & Saunders (1991) presented a correlation between  $Q_{\text{jet}}$  and the narrow line luminosity  $L_{\text{NLR}}$ . A correlation between the optical and low-frequency radio luminosities has been confirmed for a sample of steep-spectrum quasars (Serjeant et al. 1998; Willott et al. 1998), which seems to argue against the narrow line emission being controlled mainly by the environment (Dunlop & Peacock 1993).

The different angles between the radio jet axis and the line of sight can alter the observational phenomena dramatically. Radio galaxies and radio-loud quasars are believed to be the same objects viewed at different angles to the jet axis (Scheuer 1987; Barthel 1989; Antonucci 1993). A dusty torus perpendicular to the jet axis and can obscure the central emission region if the angle between the jet axis and the line of sight is large enough. The narrow line region in quasars is extended beyond the putative dusty torus, so that it is believed to be independent of the jet axis and is therefore isotropic.

Cao & Jiang (1999) have performed statistic analyses on the correlation between the total radio and broad-line emission for a sample of radio-loud quasars. The broad-line region is ionized by the central source and is therefore a good indicator of emission from the accretion disc. The broad-line data are usually easily available compared with the narrow line data which is available only for the sources within a restricted redshift range. VLA observations can separate the extended radio emission from the core emission. In this work, we use Cao & Jiang’s sample and collect all available data of extended radio emission from the literature to explore the relation between extended radio emission and broad-line emission.

We describe the adopted sample in next section. Sections 3 and 4 contain the results and a discussion. The cosmological parameters  $H_0 = 50 \text{ kms}^{-1} \text{ Mpc}^{-1}$  and  $q_0 = 0.5$  have been adopted in this work.

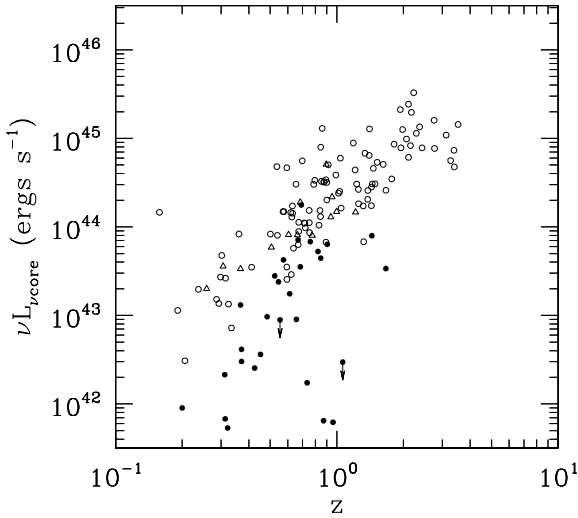


**Figure 1.** The radio core luminosity, redshift plane for the sample. The open circles represent core-dominated quasars, and the full circles represent lobe-dominated quasars, while the triangles represent BL Lac objects.

## 2 THE SAMPLE

We start with the sample of Cao & Jiang (1999), since the broad-line data of their sample have been well compiled. Their sample is a combination of all quasars and BL Lac objects with available line data in 1 Jy, S4 and S5 catalogues. The radio flux density limit of S5 catalogue at 5 GHz is 0.25 Jy. There are 198 sources in their sample including 184 quasars and 14 BL Lac objects. Their sample is drawn from the parent flux-limited sample selected at 5 GHz. The selection effects may be introduced, i.e., those sources without published line flux measurements are likely to be biased towards those with weak lines. We believe it would not affect the main results of present investigation. We search the literature and collect all available data of VLA observations on the sources, and find 141 sources with both core and extended emission data including 128 quasars and 13 BL Lac objects. The core and extended flux density is K-corrected to 5 GHz in the rest frame of the source assuming  $\alpha_c = 0$  and  $\alpha_e = -1$  ( $f_{\text{core}} \propto \nu^{\alpha_c}$ ,  $f_{\text{ext}} \propto \nu^{\alpha_e}$ ). The core and extended radio flux density at 5 GHz in the rest frame of the sources are listed in Table 1. The ratio  $R$  of the core to extended radio luminosity in the rest frame of the sources is then available (see column (6) of Table 1). The flux of narrow line [O III] is also listed in Table 1, since it is the most frequently observed narrow line for the sources in present sample. The total broad-line flux is estimated by Cao & Jiang (1999) using the line ratios reported by Francis et al. (1991).

## 3 RESULTS

We present the core and extended radio luminosity at 5 GHz in the rest frame of the source as functions of redshift  $z$  for the sample in Figs. 1 and 2. We note that the extended ra-

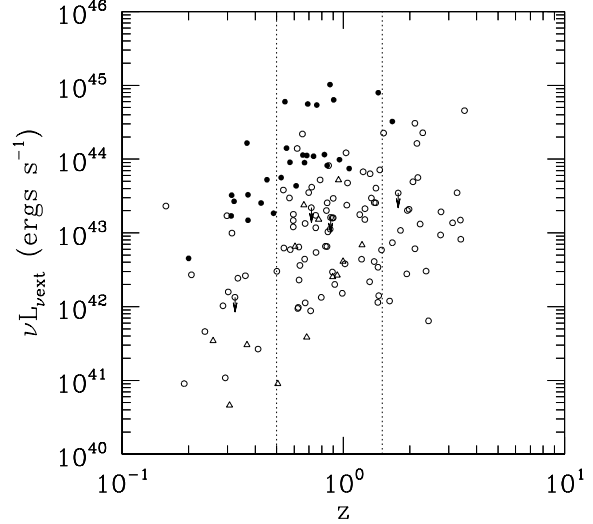


**Figure 2.** Same as Fig. 1, but for the extended radio luminosity. The restricted redshift range:  $0.5 < z < 1.5$ , is indicated by the dotted lines.

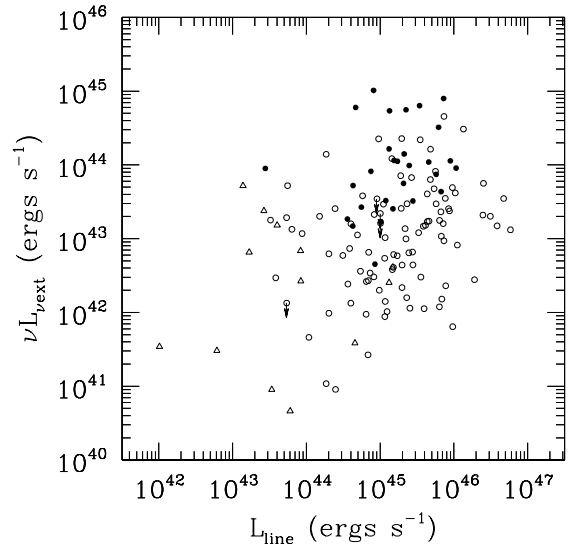


**Figure 3.** The extended radio and broad-line luminosity relation (Symbols as in Fig. 1).

dio luminosity provides wider dispersion and show weaker dependence of redshift than the core luminosity. This is due to the fact that present sample has a limit on total radio flux density, not on extended radio flux density. We plot the relation between the extended radio luminosity and total broad-line luminosity in Fig. 3 and find a significant correlation between them at  $> 99.9$  per cent confidence (Spearman correlation coefficient  $\rho$ ). It is well known that the correlation between luminosities may be caused by common redshift dependence. We therefore perform a statistic analysis on the sources in the restricted redshift range  $0.5 < z < 1.5$ . For

**Table 1.** Radio and line data of the sample.

Source (1)	Class. (2)	$z$ (3)	$f_{core}$ (mJy) (4)	$f_{ext}$ (mJy) (5)	$R$ (6)	Ref. (7)	$\log f_{[OIII]}$ (8)	Ref. (9)
0014+813	Q	3.384	162.2	3.3	49.15	K86		
0056-001	Q	0.717	773.6	<154.4	>5.01	BM87	-13.96	JB91
0106+013	Q	2.107	1560.9	196.5	7.94	BM87		
0112-017	Q	1.381	425.9	42.59	10.0	BM87		
0119+041	Q	0.637	521.5	32.9	15.85	BM87	-14.68	JB91
0133+207	Q	0.425	55.15	551.5	0.1	BM87	-13.54	JB91
0134+329	Q	0.367	389.1	4898.1	0.08	BM87	-13.08	JB91
0135-247	Q	0.831	530.5	33.47	15.85	BM87	-14.03	JB91
0159-117	Q	0.669	515.3	36.0	14.31	WB86	-13.89	T93
0212+735	Q	2.367	667.1	1.5	444.7	NH90		
0229+131	Q	2.065	660.4	33.1	19.95	BM87		
0234+285	Q	1.210	975.4	9.75	100.0	BM87		
0235+164	BL	0.940	501.0	10.3	48.64	Mu93		
0237-233	Q	2.224	1866.6	7.5	248.9	NH90	-14.47	B94
0248+430	Q	1.316	317.6	4.0	79.4	BP86		
0256+075	Q	0.893	291.6	12.8	22.78	Mu93		
0336-019	Q	0.852	1572.5	49.73	31.62	BM87		
0400+258	Q	2.109	391.0	3.91	100.0	BM87		
0403-132	Q	0.571	1715.1	342.2	5.01	BM87	-14.41	M96
0405-123	Q	0.574	482.8	1030.0	0.47	M93	-13.35	M96
0420-014	Q	0.915	2068.4	8.23	251.3	BM87		
0440-003	Q	0.844	641.5	32.15	19.95	BM87	-14.70	JB91
0458-020	Q	2.286	610.2	121.8	5.01	BM87		
0518+165	Q	0.759	422.4	3355.6	0.13	BM87	-13.96	JB91
0528-250	Q	2.765	268.06	6.73	39.83	BM87		
0537-441	BL	0.896	2185.5	10.95	199.6	BM87		
0537-286	Q	3.119	289.3	3.64	79.48	BM87		
0538+498	Q	0.545	304.5	7648.7	0.04	BM87	-13.50	L96
0539-057	Q	0.839	761.3	100.0	7.61	U81	-15.15	SK93
0602-319	Q	0.452	68.9	1000.0	0.07	U81	-13.79	R84
0605-085	Q	0.872	1467.0	51.4	28.54	BP86		
0607-157	Q	0.324	517.8	<51.78	>10.0	BM87		
0637-752	Q	0.654	2599.7	1880.0	1.38	WB86	-13.27	W99
0642+449	Q	3.396	104.4	1.8	58.0	NH90		
0711+356	Q	1.620	588.9	1.38	426.7	Mu93		
0723+679	Q	0.846	216.7	400.0	0.54	U81	-14.59	L96
0736+017	Q	0.191	1331.7	10.58	125.9	BM87	-14.12	T93
0738+313	Q	0.631	1321.3	21.3	62.03	Mu93	-14.44	JB91
0740+380	Q	1.063	<8.76	220.0	<0.04	BM87		
0804+499	Q	1.433	264.3	1.74	151.9	Mu93		
0809+483	Q	0.871	2.96	4695.2	0.0006	BM87	-13.68	L96
0814+425	BL	0.258	1248.8	21.5	58.08	Mu93		
0820+225	BL	0.951	823.2	197.7	4.16	Mu93		
0823+033	BL	0.506	879.8	1.34	656.6	Mu93		
0825-202	Q	0.822	274.4	600.0	0.46	U81	-13.98	d94
0834-201	Q	2.752	563.7	3.3	170.8	NH90		
0836+710	Q	2.172	1180.0	33.78	34.93	Mu93		
0838+133	Q	0.684	275.5	871.1	0.32	BM87	-14.91	M96
0842-754	Q	0.524	387.1	777.6	0.5	M93	-13.86	T93
0850+581	Q	1.322	123.8	115.5	1.07	BP86		
0851+202	BL	0.306	1562.0	2.0	781.0	K92	-14.85	S89
0858-279	Q	2.152	507.6	100.0	5.08	U81		
0859-140	Q	1.339	1202.0	52.6	22.85	BP86		
0859+470	Q	1.462	668.2	104.0	6.43	Mu93		
0906+015	Q	1.018	781.3	12.38	63.11	BM87		
0906+430	Q	0.668	583.2	734.2	0.79	BM87	-14.66	L96
0917+624	Q	1.446	455.8	2.1	217.1	Mu93		
0923+392	Q	0.698	4149.2	261.8	15.85	BM87	-13.06	L96
0945+408	Q	1.252	545.3	31.2	17.48	Mu93		
0953+254	Q	0.712	787.4	6.25	125.98	BM87		

**Table 1** – *continued* Radio and line data of the sample.

0954+556	Q	0.901	1350.9	125.0	10.81	Mu93	-14.33	L96
0954+658	BL	0.367	994.9	9.0	110.5	K92	-15.47	L96
1007+417	Q	0.6123	173.7	430.0	0.4	WB86	-14.51	M96
1040+123	Q	1.029	801.9	386.7	2.07	Mu93		
1045–188	Q	0.595	268.6	188.0	1.43	BP86	-14.47	S93
1055+018	Q	0.892	1481.5	69.1	21.44	BP86		
1100+772	Q	0.3115	89.75	712.9	0.13	BM87	-13.43	M96
1111+408	Q	0.734	11.55	729.1	0.02	BM87	-13.68	JB91
1127–145	Q	1.187	2051.6	40.93	50.12	BM87		
1136–135	Q	0.554	<109.4	1730.0	<0.06	WB86	-13.39	T93
1137+660	Q	0.6563	76.74	966.04	0.08	BM87	-14.52	M96
1148–001	Q	1.982	927.2	15.4	60.21	BP86		
1150+497	Q	0.334	261.6	88.0	2.97	S98	-14.03	SM87
1226+023	Q	0.158	25254.0	4002.6	6.31	BM87	-12.38	W99
1229–021	Q	1.045	500.7	145.8	3.43	H83		
1237–101	Q	0.753	542.7	34.2	15.87	BM87		
1250+568	Q	0.321	21.1	1055.3	0.02	BM87	-13.37	JB91
1253–055	Q	0.536	6326.0	502.5	12.59	BM87	-14.56	M96
1258+404	Q	1.6656	36.76	351.8	0.1	H83		
1302–102	Q	0.286	763.6	51.68	14.78	L94	-14.02	M96
1308+326	BL	0.997	505.8	14.0	36.13	K92		
1328+307	Q	0.846	3887.9	125.0	31.1	K90	-13.89	GW94
1334–127	Q	0.539	1046.0	81.3	12.87	BP86		
1340+606	Q	0.961	2.29	362.6	0.01	BM87		
1354+195	Q	0.720	680.0	290.0	2.34	WB86		
1355–416	Q	0.313	28.2	1347.0	0.02	M93	-13.70	T93
1416+067	Q	1.439	119.9	1198.8	0.1	BM87		
1424–418	Q	1.522	713.7	300.0	2.38	U81		
1442+101	Q	3.5305	288.9	91.36	3.16	BM87		
1451–375	Q	0.314	1088.3	410.0	2.65	WB86		
1458+718	Q	0.905	268.02	2680.2	0.1	BM87	-13.89	L96
1504–166	Q	0.876	1462.7	<73.3	>19.95	BM87		
1510–089	Q	0.361	2550.1	80.64	31.62	BM87	-13.91	T93
1512+370	Q	0.371	87.5	430.0	0.2	WB86	-13.77	M96
1532+016	Q	1.435	427.7	5.2	82.25	BM87		
1538+149	BL	0.605	828.7	66.3	12.5	Mu93		
1546+027	Q	0.412	812.3	6.17	131.7	Mu93	-14.01	B89
1555+001	Q	1.770	330.47	<33.0	>10.01	BM87		
1611+343	Q	1.401	1027.2	40.89	25.12	BM87		
1622–253	Q	0.786	1735.7	300.0	5.79	U81		
1633+382	Q	1.814	772.18	9.72	79.44	BM87		
1637+574	Q	0.750	976.0	110.0	8.87	K90	-14.06	M96
1638+398	Q	1.666	282.1	8.0	35.26	K90		
1641+399	Q	0.594	4923.1	155.7	31.62	BM87	-14.28	L96
1642+690	Q	0.751	708.7	74.46	9.52	S98	-15.00	L96
1704+608	Q	0.371	120.0	953.1	0.13	BM87	-12.95	W99
1721+343	Q	0.206	306.8	270.0	1.14	WB86	-12.50	W99
1725+044	Q	0.293	650.5	5.17	125.8	BM87	-13.93	R84
1739+522	Q	1.379	339.7	6.78	50.1	BM87		
1803+784	BL	0.684	1472.7	3.0	490.9	K92	-14.89	L96
1823+568	BL	0.664	673.1	198.0	3.4	K92	-15.28	L96
1828+487	Q	0.691	1345.8	4255.7	0.32	BM87	-13.55	L96
1830+285	Q	0.594	371.4	127.5	2.91	H92		
1928+738	Q	0.302	2132.0	71.0	30.03	K90	-12.46	L96
1954–388	Q	0.626	1218.0	9.2	132.4	M97		
1954+513	Q	1.230	652.0	144.0	4.53	K90		
2029+121	BL	1.215	323.0	15.1	21.39	BP86		
2126–158	Q	3.266	134.6	8.4	16.02	NH90		
2128–123	Q	0.501	1266.0	46.0	27.52	M97	-13.56	T93
2134+004	Q	1.936	1641.0	2.16	759.7	Mu93		
2135–147	Q	0.200	95.7	479.6	0.2	BM87	-12.97	W99
2136+141	Q	2.427	365.6	0.3	1218.7	NH90		
2145+067	Q	0.990	1334.7	5.25	254.3	Mu93		
2155–152	Q	0.672	717.7	108.4	6.62	W84	-14.97	S89

**Table 1** – *continued* Radio and line data of the sample.

2201+315	Q	0.298	1249.2	788.2	1.58	BM87	-13.86	M96
2203-188	Q	0.619	1402.0	1348.0	1.04	M97	-14.06	S89
2209+080	Q	0.484	158.4	303.0	0.52	H92		
2216-038	Q	0.901	857.5	68.11	12.59	BM87		
2223-052	Q	1.404	2037.2	64.42	31.62	BM87		
2223+210	Q	1.949	598.8	15.4	38.88	Mu93		
2230+114	Q	1.037	1867.7	74.35	25.12	BM87		
2234+282	Q	0.795	1880.4	7.49	251.19	BM87	-14.82	JB91
2240-260	BL	0.774	475.8	90.6	5.24	C99		
2243-123	Q	0.630	1601.0	59.8	26.77	M97	-14.14	T93
2247+140	Q	0.237	1469.0	34.3	42.83	BP86	-13.70	GW94
2251+158	Q	0.859	6128.3	386.7	15.85	BM87	-13.68	JB91
2318+049	Q	0.623	276.0	9.0	30.66	BP86		
2319+272	Q	1.253	374.6	43.7	8.57	BP86		
2328+107	Q	1.489	427.88	8.2	52.18	Mu93		
2344+092	Q	0.673	907.25	9.07	100.0	BM87	-13.21	JB91
2345-167	Q	0.576	1678.9	66.84	25.12	BM87	-14.19	JB91

Notes for the table 1. Q: quasars; BL: BL Lac objects.

Column (1): IAU source name. Column (2): classification of the source. Column (3): redshift. Column (4): core flux density in the rest frame of the source. Column (5): extended flux density in the rest frame of the source. Column (6): ratio  $R$  of the core to extended emission. Column (7): references for the radio emission. Column (8): flux of [OIII] (in ergs.  $s^{-1} \text{ cm}^{-2}$ ). Column (9): references for the line emission.

References:

B89: Baldwin et al. (1989). B94: Baker et al. (1994). BM87: Browne & Murphy (1987). BP86: Browne & Perley (1986). C99: Cassaro et al. (1999). d94: di Serego Alighieri et al. (1994). GW94: Gelderman & Whittle (1994). H83: Hintzen et al. (1983). H92: Hooimeyer et al. (1992). JB91: Jackson & Browne (1991). K86: Kühr et al. (1986). K90: Kollgaard et al. (1990). K92: Kollgaard et al. (1992). L94: Lister et al. (1994). L96: Lawrence et al. (1996). M93: Morganti et al. (1993). M96: Marziani et al. (1996). M97: Morganti et al. (1997). Mu93: Murphy et al. (1993). NH90: Neff & Hutchings (1990). R84: Rudy (1984). S89: Stickel et al. (1989). S93: Stickel et al. (1993). S98: Saikia et al. (1998). SK93: Stickel & Kühr (1993). SM87: Stockton & MacKenty (1987). T93: Tadhunter et al. (1993). U81: Ulvestad et al. (1981). W84: Wardle et al. (1984). W99: Wilkes et al. (1999). WB86: Wills & Browne (1986).

this subsample of sources, we check the correlation between luminosity and redshift, and no correlation between the extended radio luminosity and redshift is found (at 15 per cent confidence, also see Fig. 2), while a significant correlation is still present at 98 per cent confidence between the extended luminosity and total broad-line luminosity. The correlation between the extended radio flux and the broad-line flux confirms these analyses on luminosities (Fig. 4). We also use the Spearman partial rank correlation method (Macklin 1982) to check the correlations. The statistic results are listed in Table 2. We note that there are significant correlations between  $\nu L_{\nu\text{ext}}$  and  $L_{\text{line}}$  independent of  $z$ . There is almost no correlation between  $\nu L_{\nu\text{ext}}$  and  $z$  independent of  $L_{\text{line}}$  either for the whole sample or the redshift restricted subsample.

The relation between the core luminosity and total broad-line luminosity is given in Fig. 5. A strong correlation is present for the CDQs in the sample, and we can see that the behaviours of CDQs and LDQs are rather different. Similar phenomena can be seen in the relation between fluxes (see Fig. 6). We re-examine such relations between radio and narrow line [O III] emission in Figs. 7 and 8, and similar results are present. The statistic results are almost same if those sources only with an upper limit on their core or extended luminosity are ruled out in the analyses. The BL Lac objects in present sample show nothing special except for their weak line emission.

## 4 DISCUSSION

The radio emission for steep-spectrum quasars is believed to be unbeamed emission from the lobes. The dominant influence on the radio luminosity is  $Q_{\text{jet}}$ , and not the large-scale radio source environment (Serjeant et al. 1998). Therefore the radio emission can be a measure of jet power  $Q_{\text{jet}}$ . The core emission in flat-spectrum quasars is strongly beamed to us, but the extended emission is not. If the difference between flat and steep-spectrum quasars is caused by the different angles between the jet orientation and the line of sight, then one can take the extended radio emission from flat-spectrum quasars as a tracer of jet power, as that for steep-spectrum quasars. The optical continuum is a good indicator of the disc surrounding a black hole for steep-spectrum quasars, since relativistic beaming does not affect the optical continuum in these sources. Thus, the radio-optical correlation gives evidence of a disc-jet link (Serjeant et al. 1998). For flat-spectrum quasars, the optical continuum may be contaminated by the beamed synchrotron emission from jets, which prevents us from using it as an indicator of accretion power. The line emission (narrow or broad lines) can alternatively be an indicator of accretion power for both flat or steep-spectrum quasars.

We present correlations between the extended radio and broad-line emission for a sample of radio-loud quasars, most of which are CDQs (99 of 128, if we define CDQs as  $R > 1$ ).

**Table 2.** Spearman partial rank correlation analysis of the correlations present between  $\nu L_{\nu\text{ext}}$ ,  $L_{\text{line}}$  and  $z$ .  $r_{AB}$  is the rank correlation coefficient of the two variables and  $r_{AB,C}$  the partial rank correlation coefficient. The significance of the partial rank correlation is equivalent to the deviation from a unit variance normal distribution if there is no correlation present.

Sample	N	Correlated variables: A,B	$r_{AB}$	$r_{AB,C}$	significance
All	141	$\nu L_{\nu\text{ext}}, L_{\text{line}}$	0.303	0.240	2.868
		$z, L_{\text{line}}$	0.438	0.402	4.983
		$\nu L_{\nu\text{ext}}, z$	0.210	0.090	1.058
within $0.5 < z < 1.5$	90	$\nu L_{\nu\text{ext}}, L_{\text{line}}$	0.246	0.255	2.417
		$z, L_{\text{line}}$	0.199	0.210	1.979
		$\nu L_{\nu\text{ext}}, z$	-0.021	-0.073	-0.679

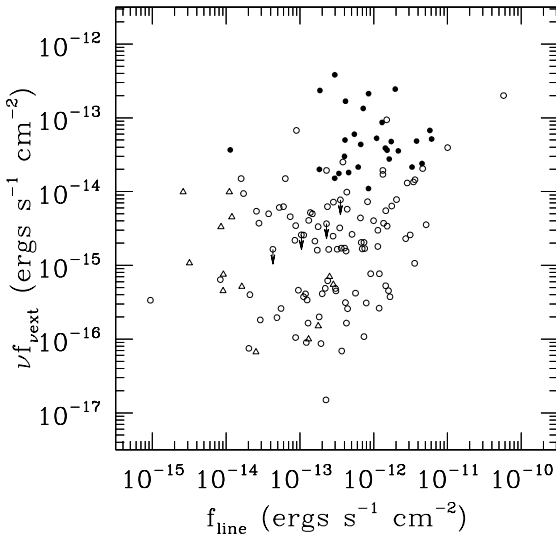


**Figure 4.** The extended radio and broad-line flux relation (Symbols as in Fig. 1).

We find significant correlations between the line emission (broad or narrow line) and extended radio emission. A significant intrinsic correlation is also found between the extended radio luminosity and total broad-line luminosity for a subsample in the restricted redshift range, while no correlation is present between the extended radio luminosity and redshift for this subsample. The Spearman partial rank correlation analyses confirm this result. We therefore believe the correlation found here is an intrinsic one which indicates a physical link between jets and accretion processes. The CDQs and LDQs follow the same statistic behaviour, while the LDQs have relatively high extended radio luminosity than their counterparts. The correlations between line and radio core emission exist for the CDQs, while the LDQs show rather different behaviours.

Another method to infer jet power is through the determination of the physical quantities of jets, such as, the Lorentz factor, the size of the jet and the density of electrons in jets, from radio and X-ray observations (Celotti & Fabian 1993). The radio emission from CDQs is beamed to us. The Doppler factor of the jet is the dominant influence on the observed radio luminosity, and radio luminosity is also determined by the size of the jet, the electron density,

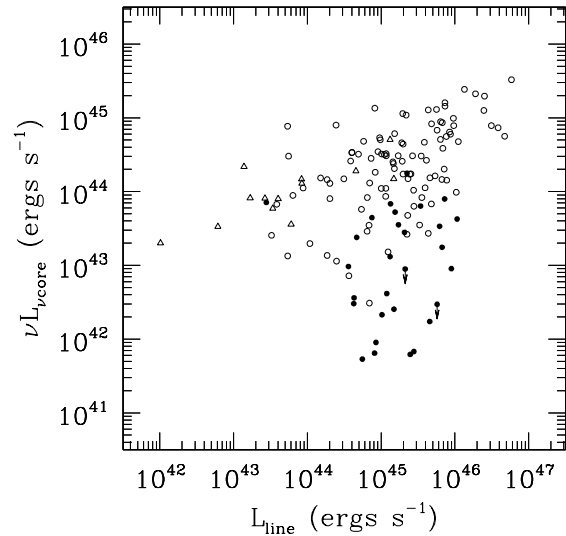


**Figure 5.** The radio core and broad-line luminosity relation (Symbols as in Fig. 1).

and the magnetic energy density in the jet. The core radio luminosity for CDQs can therefore reflect the jet power for CDQs to some extent, though the uncertainty exists on the angle between the jet axis orientation and line of sight. That might be the reason why we can also find a correlation between radio core emission and total broad-line emission for the CDQs in our sample. A similar correlation is present between the core radio emission and the narrow line [O III] emission, which seems to rule out the possibility that the correlation between the core emission and broad-line emission is caused by the orientation effect of broad-line region, i.e., a jet close to the line of sight may imply an unobstructed view of the broad-line region. It is worth pointing out that the core radio emission is not a good tracer for jet power of LDQs (see Figs. 5–8). Instead, the extended radio emission can be taken as a tracer for jet power both for CDQs and LDQs. The jet power can be derived from their extended radio luminosity based on some assumptions (see detailed discussion in Willott et al. 1999).

Similar correlation analyses are performed between radio and narrow line [O III] emission. Although the sample is reduced to a rather smaller one due to the lack of the narrow line data mainly caused by the redshift requirement on

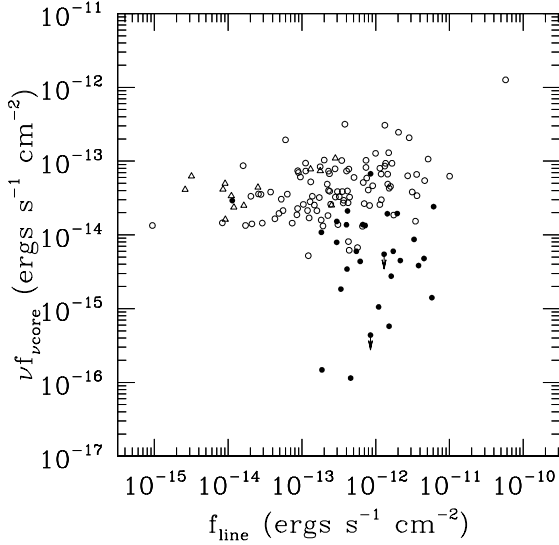


**Figure 6.** The radio core and broad-line flux relation (Symbols as in Fig. 1).

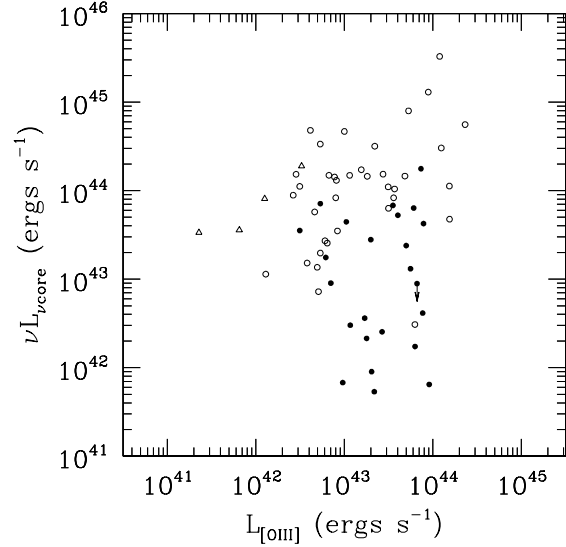


**Figure 8.** The radio core and narrow line [O III] luminosity relation (Symbols as in Fig. 1).

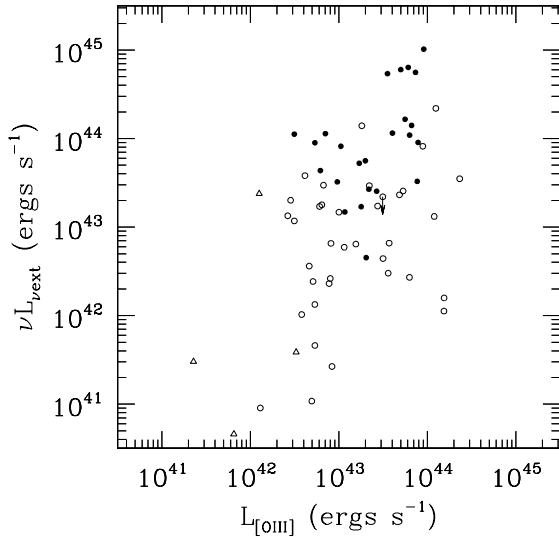


**Figure 7.** The extended radio and narrow line [O III] luminosity relation (Symbols as in Fig. 1).

observations of [O III], the similar results are present as that for the total broad-line (see Figs. 7 and 8).

#### ACKNOWLEDGMENTS

We thank Peter Scheuer and the anonymous referee for their helpful comments and suggestions. The support from the NSFC and Pandeng project is gratefully acknowledged. This research has made use of the NASA/IPAC Extragalactic Database (NED), which is operated by the Jet Propulsion Laboratory, California Institute of Technology, under con-

tract with the National Aeronautic and Space Administration.

#### REFERENCES

- Antonucci R.R.J., 1993, ARA&A, 31, 473  
 Baker A.C., Carswell R.F., Bailey J.A., Espey B.R., Smith M.G., Ward M.J., 1994, MNRAS 270, 575(B94)  
 Baldwin J.A., Wampler E.J., Gaskell C.M., 1989, ApJ, 338, 630(B89)  
 Barthel P.D., 1989, ApJ, 336, 606  
 Baum S.A., Heckman T.M., 1989, ApJ, 336, 702  
 Blandford R. D., Payne D. G., 1982, MNRAS, 199, 883  
 Blandford R. D., Znajek R. L., 1977, MNRAS, 179, 433  
 Browne I.W.A., Murphy D.W., 1987, MNRAS, 226, 601(BM87)  
 Browne I.W.A., Perley R.A., 1986, MNRAS, 222, 149(BP86)  
 Cao X., Jiang D.R., 1999, MNRAS, 307, 802  
 Cassaro P., Stanghellini C., Bondi M., Dallacasa D., Ceca R.D., Zappala R.A., 1999, A&AS, 139, 601(C99)  
 Celotti A., Fabian A.C., 1993, MNRAS, 264, 228  
 di Serego Alighieri S., Danziger I.J., Morganti R., Tadhunter C.N., 1994, MNRAS, 269, 998(d94)  
 Dunlop J.S., Peacock J.A., 1993, MNRAS, 263, 93  
 Falcke H., Biermann P., 1995, A&A, 293, 665  
 Francis P.J., Hewett P.C., Foltz C.B., Chaffee F.H., Weymann R.J., Morris S.L., 1991, ApJ, 373, 465  
 Gelderman R., Whittle M., 1994, ApJS, 91, 491(GW94)  
 Hintzen P., Ulvestad J., Owen F., 1983, AJ, 88, 709(H83)  
 Hooimeyer J.R.A., Schilizzi R.T., Miley G.K., Barthel P.D., 1992, A&A, 261, 25(H92)  
 Jackson N., Browne I.W.A., 1991, MNRAS, 250, 414(JB91)  
 Koide S., Shibata K., Kudoh T., 1999, ApJ, 522, 727  
 Kollgaard R.I., Wardle J.F.C., Roberts D.H., 1990, AJ, 100, 1057(K90)  
 Kollgaard R.I., Wardle J.F.C., Roberts D.H., Gabuzda D.C., 1990, AJ, 104, 1687(K92)  
 Kühn H., Stocke J.T., Strittmatter P.A., Bartel N., 1986, ApJ, 302, 52(K86)

- Lawrence C.R., Zucker J.R., Readhead A.C.S., Unwin S.C., Pearson T.J. et al., 1996, *ApJS*, 107, 541(L96)
- Lister M.L., Gower A.C., Hutchings J.B., 1994, *AJ*, 108, 821(L94)
- Macklin J.T., 1982, *MNRAS*, 199, 1119
- Marziani P., Sulentic J.W., Dultzin-Hacyan D., Calvani M., Mole M., 1996, *ApJS*, 104, 37(M96)
- McCarthy P.J., 1993, *ARA&A*, 31, 639
- Morganti R., Killeen N.E.B., Tadhunter C.N., 1993, *MNRAS*, 263, 1023(M93)
- Morganti R., Oosterloo T.A., Reynolds J.E., Tadhunter C.N., Migenes V., 1997, *MNRAS*, 284, 541(M97)
- Murphy D.W., Browne I.W.A., Perley R.A., 1993, *MNRAS*, 264, 298(Mu93)
- Neff S.G., Hutchings J.B., 1990, *AJ*, 100, 1441(NH90)
- Rawlings S. G., Saunders R. D. E., 1991, *Nat*, 349, 138
- Rawlings S. G., Saunders R. D. E., Eales S.A., Mackay C.D., 1989, *MNRAS*, 240, 701
- Rudy R.J., 1984, *ApJ*, 284, 33(R84)
- Saikia D.J., Holmes G.F., Kulkarm A.R., Salter C.J., Garrington S.T., 1998, *MNRAS*, 298, 877(S98)
- Scheuer P.A.G., 1987, in Zensus J.A., Pearson T.J., eds, *Superluminal Radio Sources*. Cambridge Univ. Press, Cambridge, p. 331
- Serjeant S., Rawlings S., Maddox S.J., Baker J.C., Clements D., Lacy M., Lilje P.B., 1998, *MNRAS*, 294, 494
- Stickel M., Kühr H., 1993, *A&AS*, 101, 521(SK93)
- Stickel M., Fried W., Kühr H., 1989, *A&AS*, 80, 103(S89)
- Stickel M., Kühr H., Fried W., 1993, *A&AS*, 97, 483(S93)
- Stockton A., MacKenty J.W., 1987, *ApJ*, 316, 584(SM87)
- Tadhunter C.N., Morganti R., Alighieri S. et al., 1993, *MNRAS*, 263, 999(T93)
- Tadhunter C.N., Morganti R., Robinson A., Dickson R., Villar-Martin M., Fosbury R.A.E., 1998, *MNRAS*, 298, 1035
- Ulvestad J., Johnston K., Perley R., Fomalont E., 1981, *AJ*, 86, 1010(U81)
- Wardle J.F.C., Moore R.L., Angel J.R.P., 1984, *ApJ*, 279, 93(W84)
- Wilkes B.J., Kuraszkiewicz J., Green P.J., Mathur S., McDowell J.C., 1999, *ApJ*, 513, 76(W99)
- Willott C.J., Rawlings S., Blundell K.M., Lacy M., 1998, *MNRAS*, 300, 625
- Willott C.J., Rawlings S., Blundell K.M., Lacy M., 1999, *MNRAS*, 309, 1017
- Wills B.J., Browne I.W.A., 1986, *ApJ*, 302, 56(WB86)
- Xu C., Livio M., 1999, *AJ*, 118, 1169